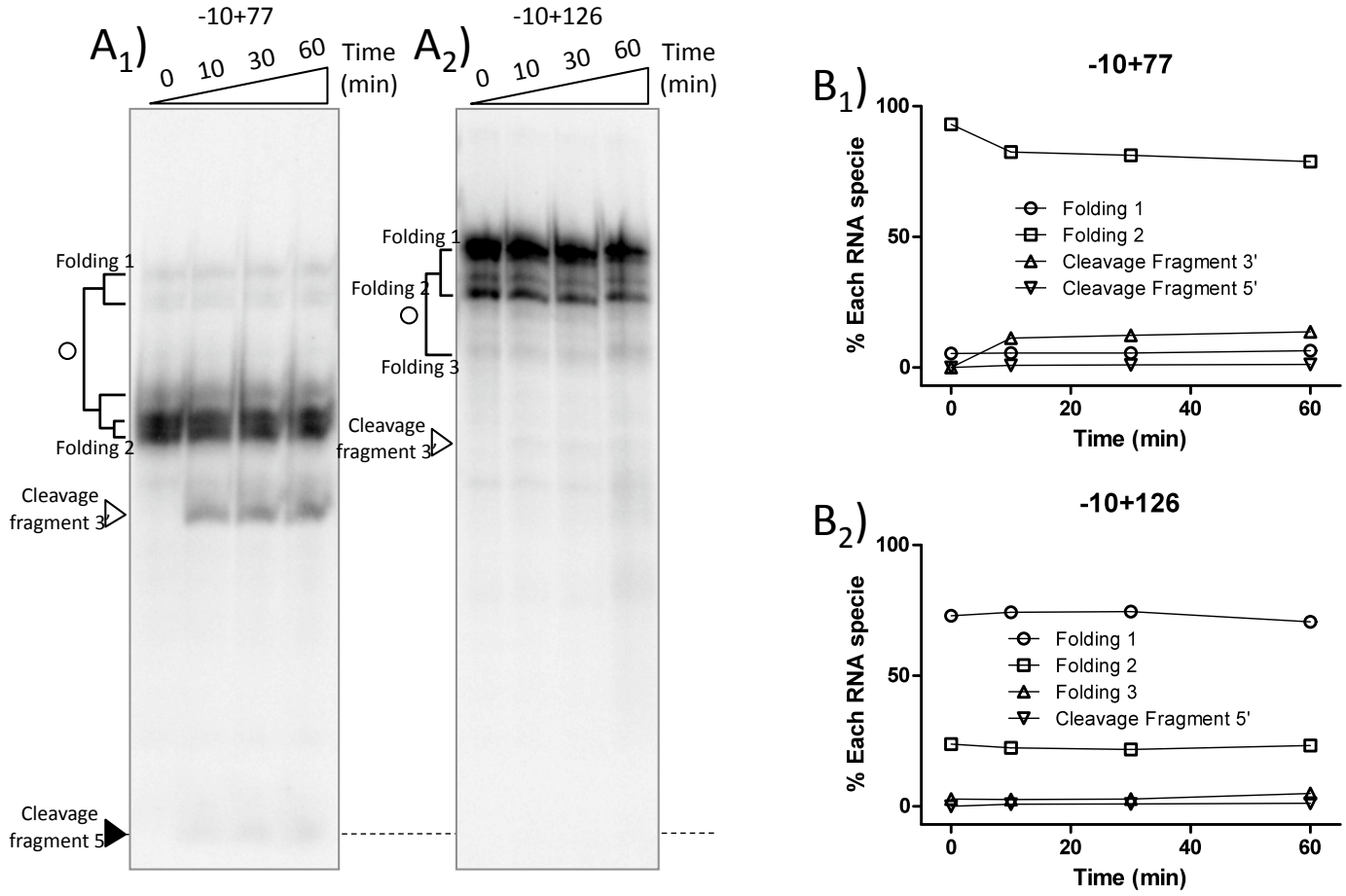

Supplementary Figure 1

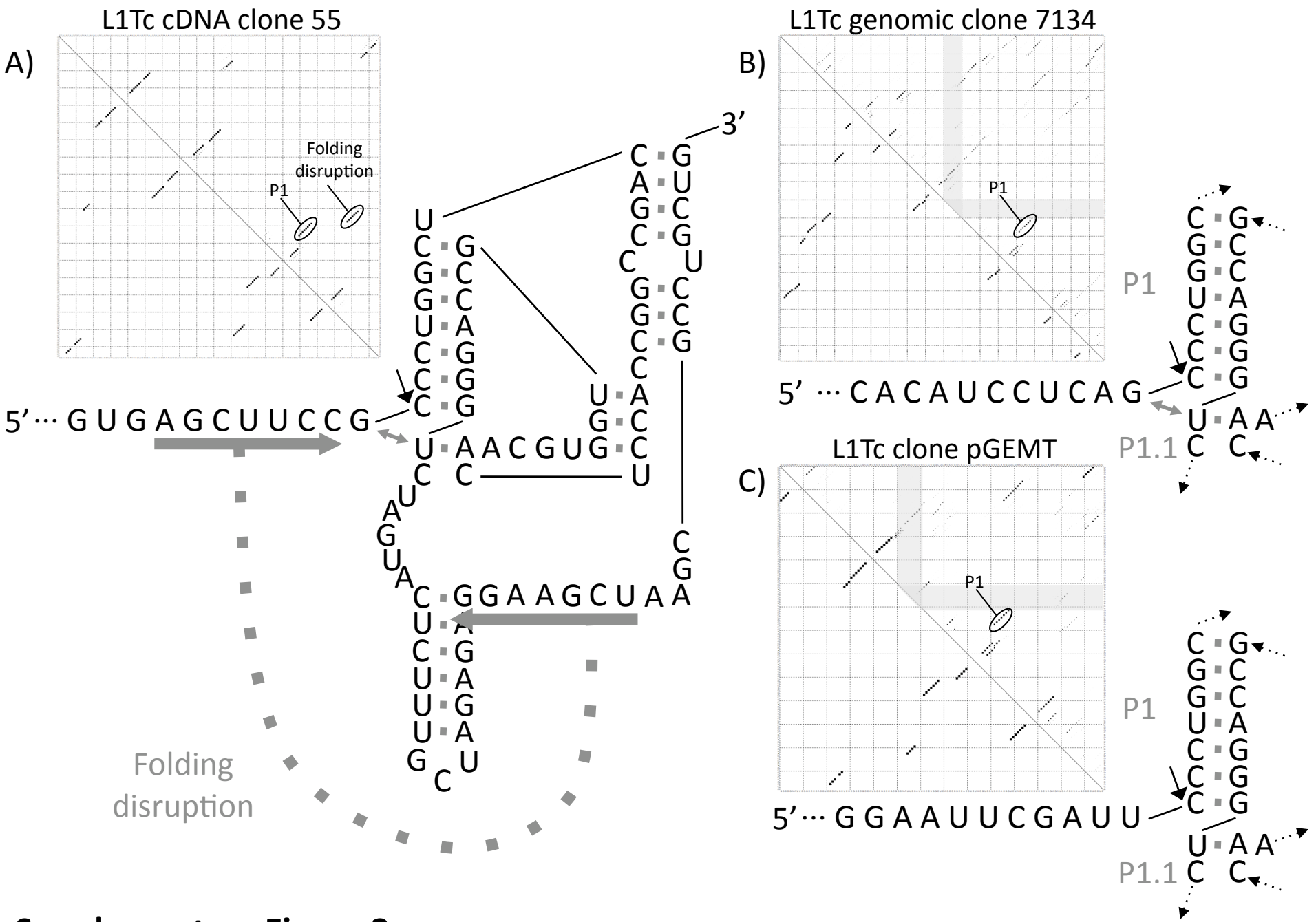

Supplementary Figure 2

Supplementary figure 1. Cleavage reaction in native gel. Post-transcriptional cleavage reactions of the constructs from clone 7134-10/L1Tc+77 (A_1), +126 (A_2) and +152 (data not shown) were performed at 1 mM Mg^{2+} concentration and 37 ºC for 0, 10, 30 and 60 minutes. Reactions were resolved by 6% poly-acrylamide, 0.25X TBE native gel electrophoresis. The uncleaved RNAs were gel-purified after transcription. The method used was as described for the kinetics reaction with the exception that each time point was prepared separately. The reactions started at different times to synchronize the end point. The folding pattern of the uncleaved RNAs is observed in lines 0 while the cleavage products are observed in lines 10, 30 and 60 minutes (A_1-A_2, empty and solid arrowheads for 3'- and 5'-products respectively). All the observed conformers and cleavage products (A_1-A_2) were quantified (B_1-B_2). Clone 7134-10/L1Tc+77 derived RNA conformers that exhibited a slower mobility, referred as folding 1, showed to be under-represented and to lack ribozyme activity. The most abundant conformation adopted by clone 7134-10/L1Tc+77 derived RNA, referred as folding 2, was cleavage-competent (A_1 and B_1). The cleavage products for clone 7134-10/L1Tc+126 derived RNA were hardly detectable (A_2, empty arrowhead). Furthermore, the particular conformer distribution adopted by the clone 7134-10/L1Tc+126 derived RNA, which showed to be enriched in the slow-migrating conformations (folding 1 and 2, A_2), did not allow us to determine the cleavage-competent conformer (B_2) since no one exhibited a reduction associable with the generation of the cleavage products. Cleavage products for clone 7134-10/L1Tc+152 derived RNA were undetectable (figure not shown). The most likely interpretation of these data is that the folding of a L1Tc region longer than 77 nt disrupts the structure adopted by the L1Tc+77 sequence and consequently its ribozyme activity, suggesting a complete RNA folding rearrangement from a ribozyme-like to a non-catalytic folding. This RNA folding rearrangement may occur when RNA elongation overtakes position +77 of L1Tc.

Supplementary figure 2. Role of the upstream nucleotides in the cleavage activity. Dotplot folding analysis performed by RNAfold software is represented together with the folding scheme predicted for each clone ribozyme: A) Clone 55-110/L1Tc+77; B) Clone 7134-100/L1Tc+77; and C) Clone pGEM-T easy-61/L1Tc+77. RNAfold analysis predicts a strong helical folding within the immediately upstream region of clone 55 with downstream nucleotides within the ribozyme core (wide arrows joined by dotted line). Both clones, 55 and 7134, allow the G_{-1}:U_{+38} wooble basepair previously described as deletereous for the cleavage (double-arrow). Immediately upstream nucleotides of 7134 and pGEM-T easy clones have not been predicted to misfold the ribozyme structure (horizontal shadowed region within dotplots), neither to adopt solid structures within the upstream region (vertical shadowed region within dotplots). pGEM-T easy clone does not allow any disruption of the P1.1 helix by elongation of P1 helix.

Supplementary table 1. Observed Rate Constants for the cleavage reaction of clone 7134 and pGEM-T easy ribozymes at 10 mM $MgCl_2$. The data of the cleavage reaction was fitted to both hyperbolic and double-exponential models. Equations are respectively $f_c = A / (t + T_{0.5})$ and $f_c = A + Be^{-k_1 t} + Ce^{-k_2 t}$. For the hyperbolic one: f_c is the cleaved fraction; Y_{max} is the cleavage fraction at infinite times; t is the time; and $T_{0.5}$ is the time at $f_c = A / 2$. For the double-exponential one: f_c is the cleaved fraction; k_1 and k_2 are the observed first-order rate constant for the fast and slow phases respectively; t is the time; A is the cleavage fraction at infinite times; and $-B$ and $-C$ are the amplitudes

of the observable phases. Plots are represented at figure 3 and are the result of three independent triplicates.

	Clone pGEM-T easy		Clone 7134	
[$MgCl_2$] (mM)	10	1	10	1
Double exponential model (two-phase decay)				
R^2	0.9994	0.9961	0.9908	0.9855
Y_0 ($^o/_1$)	-2.747×10^{-8} ± 0.00267	1.108×10^{-8} ± 0.007067	-4.523×10^{-9} ± 0.01149	0.003656 ± 0.01492
A ($^o/_1$)	0.6581 ± 0.001199	0.6745 ± 0.003125	0.7066 ± 0.005120	0.6441 ± 0.009498
k_1 (fast) (min^{-1})	~ 29231	~ 1.370×10^6	~ 178252	0.2998 ± 0.05853
k_2 (slow) (min^{-1})	0.04776 ± 0.004208	0.05048 ± 0.0.007395	0.04862 ± 0.006313	0.02255 ± 0.003929
Hyperbolic				
R^2	0.9799	0.9905	0.9955	0.9782
A ($^o/_1$)	0.6961 ± 0.006179	0.6663 ± 0.003839	0.6513 ± 0.002544	0.6513 ± 0.009042
$T_{0.5}$ (min)	1.128 ± 0.1043	0.4925 ± 0.04876	0.2771 ± 0.02880	7.824 ± 0.5934